

SMASIS2016-9242

**ROBUST SELF-SENSING IN NITI ACTUATORS
USING A DUAL MEASUREMENT TECHNIQUE**

Austin Gurley*

Department of Mechanical Engineering
Auburn University
Auburn, Alabama, USA

Tyler Ross Lambert

Department of Mechanical Engineering
Auburn University
Auburn, Alabama, USA

David Beale

Department of Mechanical Engineering
Auburn University
Auburn, Alabama, USA

Royall Broughton

Department of Polymer and Fiber Engineering
Auburn University
Auburn, Alabama, USA

ABSTRACT

Using a Shape Memory Alloy (SMA) actuator as both an actuator and a sensor provides huge benefits in cost reduction and miniaturization of robotic devices. Despite much effort, reliable and robust self-sensing (using the actuator as a position sensor) has not been achieved for general temperature, loading, hysteresis path, and fatigue conditions. Prior research has sought to model the intricacies of the electrical resistivity changes within the NiTi material. However, for the models to be solvable, nearly every previous technique only models the actuator within very specific boundary conditions. Here, we measure both the voltage across the entire NiTi wire and of a fixed-length segment of it; these dual measurements allow direct calculation of the actuator length without a material model. We review previous self-sensing literature, illustrate the mechanism design that makes the new technique possible, and use the dual measurement technique to determine the length of a single straight wire actuator under controlled conditions. This robust measurement can be used for feedback control in unknown ambient and loading conditions.

INTRODUCTION AND MOTIVATION

SMA actuators comprised simply of thin electrically heated wire can provide huge benefits in cost reduction and miniaturization of robotic devices. Much of the research on SMA actuators falls into three categories: modelling, control, and design. Because both the models and controls are very complex, SMA actuators have not become prevalent in robot or

machine design except in places where binary (two-position) motion is all that is needed. Binary control allows the model to be as simple as two known positions; the state when hot and when cold. A more useful actuator will be easily commanded to obtain a desired position (or force) anywhere within its range of capability, not just at the limits. To do this, generally a position (force) sensor is used in a feedback loop with the actuator. While sensor feedback is feasible in many cases, the great benefits of SMA actuators (high payload-to-weight ratios, simplicity, and small size) cannot usually be realized in this configuration because the added sensor adds complexity, weight and volume. Ideally the changing electrical properties of the SMA material itself could be used as a position (load) sensor. Because the behavior of the SMA motion and electrical properties are nonlinear and exhibit hysteresis, it has proven difficult to create a robust self-sensing control scheme. No previous research has successfully modeled the electrical properties accurately for general loading and ambient conditions – this is crucial for a robotic actuator since the ‘artificial muscle’ must control motion under varying loads and reject disturbances during use.

We have developed an SMA actuator dual measurement method that allows self-sensing without complex models. This method is simple, only requiring one additional voltage measurement at a stationary point along the length of the actuator, and can easily be incorporated in practical robotic devices. By making the secondary measurement, the length of the actuator can be calculated directly and accurately with no assumptions about ambient conditions or loads except that they are constant along the entire actuator length. The method is not

affected by hysteresis, twinning, or R-phase transformations which cause other methods to fail.

In this work, we begin by reviewing existing SMA resistivity modelling and attempts to self-sense accurately with NiTi actuators. While these models do seem to model the material correctly, it is found that no previous self-sensing method is robust to both unknown ambient conditions and unknown loads. Our dual measurement technique is described, and relevant equations are derived. An experiment is performed that shows the robust length sensing ability of the actuator. The dual measurement technique is compared to the use of resistance alone, and shown to be superior. The assumptions required and sources of inaccuracy are discussed.

RESISTANCE MODELING

It has been ‘common knowledge’ in the SMA community for many years that the resistance of SMA materials can be used for self-sensing of strain. However, when trying to apply the concept, it is found that strain is only one component of the resistance variation; the actual response is affected by strain, stress, temperature, and Martensite phase fraction. In many cases, the easy solution is to assume the wire position is proportional to heating power applied [1], or to operate the actuator in only two positions at the end of the travel [2, 3]. Because of the large effect of transformation on strain (compared to other terms in the constitutive model) it has been proposed in several works that the relationship between strain and resistance is sufficiently linear to use for control [6, 9]. Wu showed that the resistance vs strain relationship is very linear for super-elastic wires at constant temperature [10].

However a more general sensing technique should allow control to intermediate positions. Most researchers approach self-sensing by modelling the resistivity of the material and the change with temperature, load and crystal phase fraction. A model employed by several researchers is the linear phase-fraction model with temperature dependent coefficients. Ikuta (1991) modelled the resistivity (ρ) of an SMA wire as a function of Martensite phase fraction (ξ) [4, 5]

$$\rho = (1 - \xi)\rho_A + \xi\rho_M \quad (1)$$

Where ρ_A and ρ_M are the resistivities of the material in Austenite and Martensite phases, respectively. The resistivity of each phase is also a linear function of temperature T ;

$$\begin{aligned} \rho_A &= \rho_{A0} + \alpha_A(T - T_0) \\ \rho_M &= \rho_{M0} + \alpha_M(T - T_0) \end{aligned} \quad (2)$$

Where T_0 is the temperature at which the initial/reference resistivity, ρ_{M0} and ρ_{A0} , is measured. We have removed the additional term that is typically included for R-phase; R-phase transformation confuses many experimental results as it seems to behave macroscopically like Martensite, but has very different electrical resistivity than either Martensite or Austenite. It has been demonstrated in many cases that

transformation to the R-phase can be precluded by maintaining actuator stress above ~ 150 MPa (e.g. [6]). It can also be eliminated by shape-setting at high temperatures, though this may have other adverse effects [7]. To be certain the resistance change is due to crystal transformation and not another mechanism, Antonucci confirmed the effect of the crystal phases on resistivity using differential scanning calorimetry [8].

However, attempts at self-sensing with varying temperatures and stresses further complicates the model. Novak uses a similar model to Ikuta and adds a term for stress [11]

$$\begin{aligned} \rho_A &= \rho_{A0} + \alpha_A(T - T_0) + \beta_A\sigma \\ \rho_M &= \rho_{M0} + \alpha_M(T - T_0) + \beta_M\sigma \end{aligned} \quad (3)$$

These equations again ignore the R-phase components of the model in this equation, since it can be eliminated by preloading. This does indeed fit better to experimental data than the Ikuta model: In constant stress tests this makes a good model [11, 12, 13, 14]. There is, however, a realistic and more practical interpretation than the additional of a stress term; because the stress causes strain (change in length) and contraction of area (due to Poisson contraction) it is really the elastic strain that causes the additional resistance [15, 16, 17]. This can be modelled by noting [18]

$$\begin{aligned} R &= \frac{\rho l}{A} \\ \epsilon_{elastic} &= \frac{\sigma}{E} \\ l(\epsilon_{elastic}) &= l_0(1 + \epsilon_{elastic}) \\ A(\epsilon_{elastic}) &= \pi R_0^2(1 - \nu\epsilon_{elastic})^2 \end{aligned} \quad (4)$$

R is the total resistance of the wire, l its length, A the cross-sectional area, $\epsilon_{elastic}$ the elastic component of strain, and ν is the wire’s Poisson ratio.

All of these models are difficult to employ for self-sensing since they do not include any hysteresis and require knowledge of ξ and temperature which cannot be practically measured, especially for thin wire actuators. To reduce the error of neglecting hysteresis, polynomial models have been used to fit the strain vs resistance curve separately on the heating and cooling paths – but these rely on knowledge of the wire stress [1, 19, 20, 21].

A clever solution for elimination of some nonlinear error is to arrange two SMA actuators in antagonistic manner and measure the difference in resistance between them [22, 23]. However, the material behavior is different for antagonist pairs than with single wires, and requires additional consideration during implementation [24]. This method also does not sufficiently eliminate the effects of hysteresis, and cannot account for the effect of differing stress in the two antagonist wires.

A complete model of shape memory resistivity must model many aspects of the behavior to provide robust self-sensing. It must

- Be stress independent

- Account for ambient temperature
- Account for ambient air currents
- Eliminate hysteresis error
- Account for wire fatigue strain
- Not require additional measurements
- Be compatible with the alloy used
- Not require exact wire temperature

None of the self-sensing models considered to date can account for all of these important factors.

THERMAL MODELLING

An additional modelling consideration in self-sensing is thermal response. SMA actuators are typically activated by electrical heating and cooled by ambient air. Passing electric current through the wire is the practical input, but the change in temperature that drives the shape memory effect. Because SMA wires are typically very small, it is not possible to measure the temperature of the device directly unless in very specially controlled ambient conditions. Thus, a reliable model of the heat transfer between the wire and the ambient air is needed for sensing using (1-4). The temperature of the SMA wire can be estimated using the common linear heat transfer model, involving a heat transfer coefficient h , wire surface area A , wire mass m and specific heat c_p , and including an additional term for the latent heat of transformation ΔH [14, 25].

$$m(c_p + \Delta H \dot{\xi}) \frac{dT}{dt} = I^2 R(\xi) - h(\xi, T)A(T - T_\infty) \quad (5)$$

Some authors disregard the latent heat component when actuation speeds are slow. Regardless, this model will have error due to disturbances such as wind speed and unknown ambient temperature which affect $h(\xi, T)$ significantly, so should not be used directly for control.

EXPERIMENTAL SETUP

The device being tested is a simple, straight SMA wire. The physical characteristics of the wire are listed in Table 1.

Table 1- SMA actuator characteristics

Characteristic	Value
Initial (Hot) Length	160 mm
Cold Length	168.1 mm
Diameter	0.125 mm
Mass	12.6 mg
Expected A_f	90 deg C
Treatment	Kroll's Reagent
Source	Dynalloy Flexinol HT

Our measurement system is comprised of two main components. The first is a high-side measurement of voltage V_3 across and current I through the entire SMA wire. The V_3 voltage lead is soldered to the end of the SMA wire, such that it moves as the wire changes length. The second component is a set of two voltage probes (V_1 and V_2), set a fixed distance (l_0) from the stationary end of the wire and a fixed distance from each-other (l_s). The set of two probes making sliding contact with the SMA wire on a 1.5mm Chrome-plated steel cylinder. These probes are mounted on a plate in the testing machine such that they can be moved up and down to change l_0 .

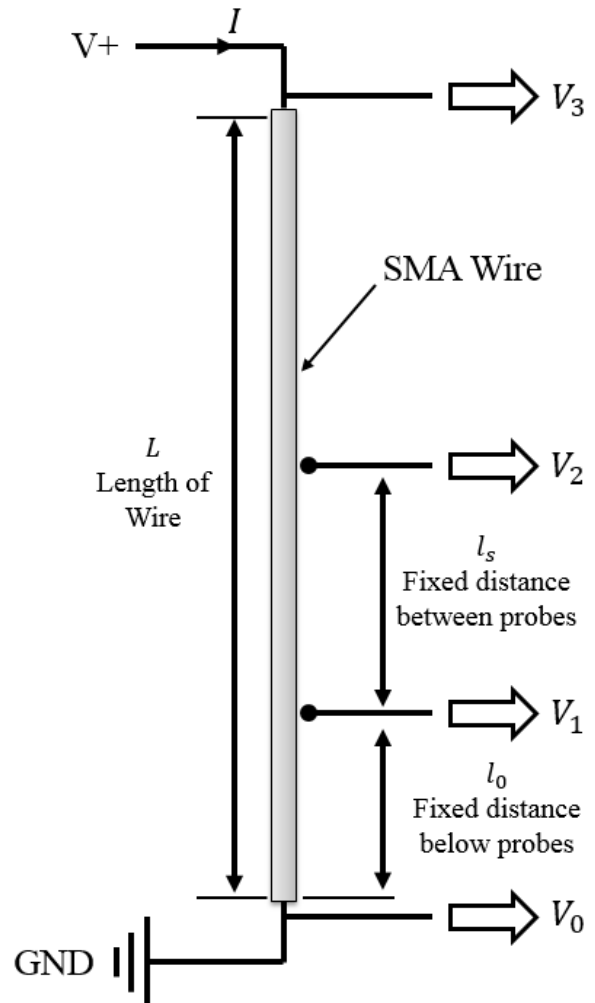


Figure 1 – Experiment Setup Schematic

The experiment is performed on a custom-built tensile testing machine. This machine controls the electrical input to the SMA actuator, and simulates a system for the SMA actuator to control. In this experiment, the simulated system is a simple suspended mass in earth gravity. Electric current is controlled through the SMA wire in a slow saw-tooth manner, and the load is regulated. Three simulated masses are used; 100 gm, 200 gm,

and 300 gm. By repeating the test with these different loads, we will see that the model can estimate actuator length regardless of the stress applied – a valuable result for robust sensing. The ambient temperature is approximately 25 deg C throughout the duration of the test, though no enclosure is provided to limit air currents since that is not typically realistic for general actuators.

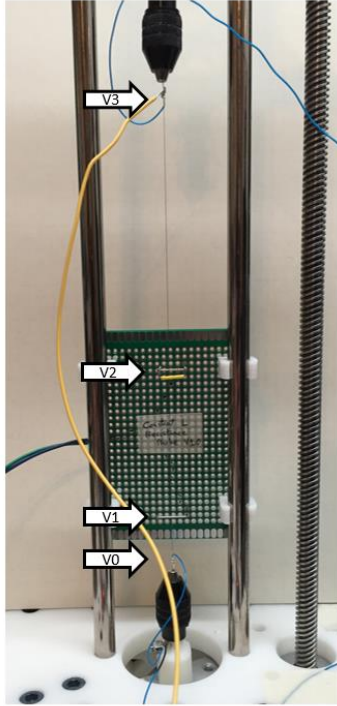


Figure 2 - Tensile Testing Machine and Experimental Setup

The initial position, with the wire completely heated is listed in Table 2. The lower distance l_0 can be adjusted, but is kept constant in these experiments.

Table 2- SMA actuator parameters required for length calculations

Distance	Value
L	160 mm
l_s	55 mm
l_0	91 mm

CALCULATIONS

The useful quantities that can be computed using the dual measurement are now presented. It is easily shown that, if l_s and l_0 are constant, then

$$L = l_0 + l_s * \frac{V_3 - V_1}{V_2 - V_1} \quad (6)$$

Thus we can directly solve for actuator length with no knowledge of the actuator properties besides initial length and slider position, nor a model of the material. This is only

accurate if the material properties are equal along the entire length of the wire, thus it provides a better estimate for larger l_s . Because sensor noise is unavoidable, it is best to maximize the denominator in (6) by having l_s as large as is practical, and l_0 as small as is practical. Thus, if possible, V_1 should be measured at ground ($l_0 = 0$), and l_s should be as close to the contracted length of the wire as possible. This also reduces inaccuracies arising due to varying conditions along the length of the wire. If these recommendations are made, then the model reduces to

$$L = \frac{l_s V_3}{V_2} \quad (7)$$

The electrical resistivity (with units Ohm*m) is easily calculated using

$$\rho = \frac{A (V_2 - V_1)}{l_s I} \quad (8)$$

RESULTS

The experimental results validate the dual measurement technique. The experiment is performed in 3 parts. The driving input is SMA current, driven from 40 to 250 mA in a saw-tooth manner, and the load is regulated to 300, 200 and 100 gf during three current sweeps (Figure 3). The stresses due to these loads are approximately 80, 160, and 240 MPa, respectively. Before each new load, the actuator is allowed to stabilize at the new equilibrium position – measurements during this transition are not recorded (causing data discontinuity at 40 and 80 seconds).

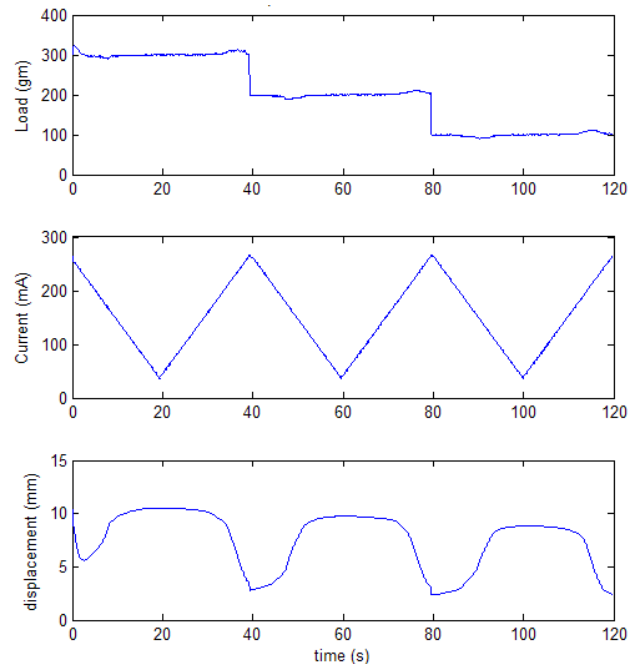


Figure 3 - Driving inputs for the experiment are three loads held constant (top) while current is swept in a saw-tooth manner (middle) which extends and contracts the actuator (bottom)

The test shows the inadequacy of assuming the resistance directly relates to actuator strain; electrical resistance is plotted against actuator length in Figure 4. Several observations can be made about this plot;

- The main trend is linear
- There is large hysteresis when near 100% Martensite (longest length)
- There is a very wide hysteresis band at low load (100 gf)
- The R vs strain relationship reverse near the ends due to temperature

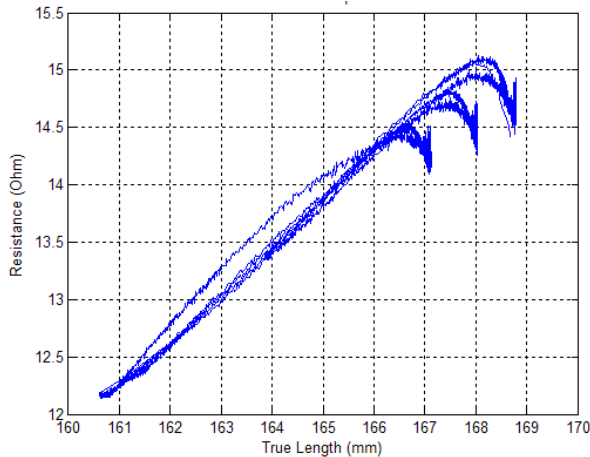


Figure 4 - Resistance of the SMA wire, by itself, makes a poor displacement sensor due to combined effects of elastic strain, temperature, and shape memory hysteresis.

By computing a length estimate using (6), we can directly calculate the actuator length as seen in Figure 5. The estimate is very linear and matches well to the measured position. The estimate becomes accurate as soon as the wire touches the probe – this can be seen in the middle of the plot as the wire initially heats and contacts the sliding probe (near 165 mm).

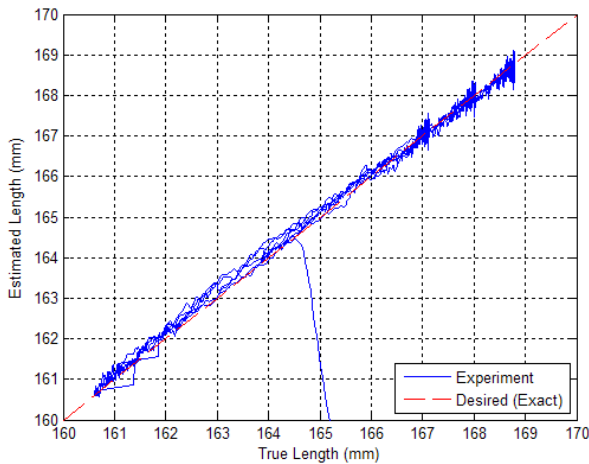


Figure 5 - Position estimated using the dual measurement technique

DISCUSSION & CONCLUSION

In more than 30 repeated tests, the measurement error is typically banded within 0.5 mm of the true length. This is true even as the wire shows permanent deformation with repeated cycling. Error is calculated by subtracting the estimated length from the true length; the error in all experiments show RMS error below 0.033 mm and standard deviation of 0.154 mm. As an actuator, we often care about the error as a percentage of the total travel, not length. With an effective stroke of 8.2 mm in the 160 mm wires used, this implies 0.4% mean and 1.88% standard deviation. The noise appears to be solely related to noise in the voltage measurements made. Hardware or software filtering can effectively improve the noise. The mean error has not physical basis, and must be a fault in the hardware calibration of the reference displacement sensor.

The dual measurement method eliminates the major sources of error in existing methods, but introduces new concerns;

- The wire surface must be conductive
- Corrosion may affect the measurement over time
- Sliding contact may reduce wire life
- Electrical noise affects result

Future work will study these potential issues. Superior surface finish of the wire could prove to eliminate corrosion and maintain electrical conductivity. Improved mechanical design of the sliding contact can eliminate wear – techniques from electric motors and slip rings may be adopted for this purpose. Electrical noise is directly related to the quality of the ADC and the level of filtering used. In situations where the sample rate is fast compared to the required sensing bandwidth, software or hardware filtering can significantly eliminate the noise.

The dual measurement technique has allowed us to estimate the length of a general SMA wire without prior knowledge of

- The wire electro-mechanical properties
- Loading and temperature conditions
- Ambient conditions
- The electric current in the wire

Thus we have created a robust mechanism for self-sensing in SMA actuators for use in robotics applications. Without a sensor for feedback, accurate robots cannot be built; the dual measurement technique has the potential to make SMA actuators more cost effective by eliminating the need for position sensors. It also allows the actuators to be smaller and to fit more degrees of freedom in a smaller space. Dual measurement provides a reliable and simple technique to implement robust self-sensing in SMA actuators.

ACKNOWLEDGMENTS

This work was supported by the Alabama Space Grant Consortium, NASA Training Grant NNX15AJ18H.

REFERENCES

- [1] T.-M. Wang, Z.-Y. Shi, D. Liu, C. Ma and Z.-H. Zhang, "An Accurately Controlled Antagonist Shape Memory Alloy Actuator with Self Sensing," *Sensors*, vol. 12, pp. 7682-7700, 2012.
- [2] K. Yang and C. L. Gu, "A novel robot hand with embedded shape memory alloy actuators," *Proceedings of the Institution of Mechanical Engineers - Part C - Journal of Mechanical Engineering Science*, vol. 216, pp. 737-745, 2002.
- [3] F. Simone, A. York and S. Seelecke, "Design and Fabrication of a Three-Finger Prosthetic Hand using SMA muscle wires," in *Proceedings of SPIE 9429 Bioinspiration, Biomimetics, and Bioreplication*, 2015.
- [4] K. Ikuta, M. Tsukamoto and S. Hirose, "Shape Memory Alloy Servo Actuator System with Electric Resistance Feedback and Application for Active Endoscope," in *Proceedings of 1988 International Conference on Robotics and Automation*, Philadelphia, 1988.
- [5] K. Ikuta, M. Tsukamoto and S. Hirose, "Mathematical Model and Experimental Verification of Shape Memory Alloy for Designing Micro Actuator," in *Micro Electro Mechanical Systems (MEMS '91) Proceedings. An investigation of Micro Structures, Sensors, Actuators, Machines, and Robots IEEE*, Nara, 1991.
- [6] M. Pozzi and G. Airoidi, "The electrical transport properties of shape memory alloys," *Materials Science and Engineering A*, vol. A273, no. 275, pp. 300-304, 1999.
- [7] J. Uchil, K. Ganesh Kumara and K. Mahesh, "Effect of thermal cycling on R-phase stability in a NiTi shape memory alloy," *Materials Science and Engineering A*, vol. 332, pp. 25-28, 2002.
- [8] V. Antonucci, G. Faiella, M. Giordano, F. Mennella and L. Nicolais, "Electrical resistivity study and characterization during NiTi phase transformation," *thermochimica acta*, vol. 462, pp. 64-69, 2007.
- [9] Z. He, K. Gall and L. Brinson, "Use of Electrical Resistance Testing to Redefine the Transformation Kinetics and Phase Diagram for Shape Memory Alloys," *Metallurgical and Material Transactions A*, vol. 37A, pp. 579-587, 2006.
- [10] X. D. Wu, J. S. Wu and Z. Wang, "The variation of electrical resistance of near stoichiometric NiTi during thermo-mechanic procedures," *Smart Materials and Structures*, vol. 8, pp. 574-578, 1999.
- [11] V. Novak, P. Sittner, G. Dayananda, B. Braz-Fernandes and K. Mahesh, "Electrical resistance variation of NiTi shape memory alloy wires in thermomechanical tests: Experiments and simulation," *Materials Science and Engineering A*, Vols. 481-482, pp. 127-133, 2008.
- [12] H. Song, E. Kubica and R. Gorbet, "Resistance Modelling of SMA Wire Actuators," in *International Workshop at the Smart Materials, Structures & NDT in Aerospace*, Montreal, 2011.
- [13] J. Zhang and Y. Yin, "SMA-based bionic integration design of self-sensor-actuator-structure for artificial skeletal muscle," *Sensors and Actuators A: Physical*, vol. 181, pp. 94-102, 2012.
- [14] J.-J. Zhang, Y.-H. Yin and J.-Y. Zhu, "Electrical Resistivity-Based Study of Self-Sensing Properties for Shape Memory Alloy-Actuated Artificial Muscle," *Sensors*, vol. 13, pp. 12958-12974, 2013.
- [15] D. Cui, G. Song and H. Li, "Modeling of the electrical resistance of shape memory alloy wires," *Smart Materials and Structures*, vol. 19, pp. 1-8, 2010.
- [16] N. Lewis, A. York and S. Seelecke, "Experimental characterization of self-sensing SMA actuators under

- controlled convective cooling," *Smart Materials and Structures*, vol. 22, pp. 1-10, 2013.
- [17] S. Furst and S. Seelecke, "Modeling and experimental characterization of the stress, strain, and resistance of shape memory alloy actuator wire with controlled power input," *Journal of Intelligent Material Systems and Structures*, vol. 23, no. 11, pp. 1233-1247, 2012.
- [18] S. Furst, J. Crews and S. Seelecke, "Stress, strain, and resistance behavior of two opposing shape memory alloy actuator wires for resistance-based self-sensing applications," *Intelligent Material Systems and Structures*, vol. 24, no. 16, pp. 1951-1968, 2013.
- [19] C.-C. Lan and C.-H. Fan, "An accurate self-sensing method for the control of shape memory alloy actuated flexures," *Sensors and Actuators A*, vol. 163, pp. 323-332, 2010.
- [20] C.-C. Lan, C.-M. Lin and C.-H. Fan, "A Self-Sensing Microgripper Module With Wide Handling Ranges," *IEEE/ASME Transactions on Mechatronics*, vol. 16, no. 1, pp. 141-150, 2011.
- [21] S.-H. Liu, T.-S. Huang and J.-Y. Yen, "Tracking Control of Shape-Memory-Alloy Actuators Based on Self-Sensing Feedback and Inverse Hysteresis Compensation," *Sensors*, vol. 10, pp. 112-127, 2010.
- [22] R. Josephine, N. Sunjai and K. Dhanalakshmi, "Differential resistance feedback control of a self-sensing shape memory alloy actuated system," *International Society of Automation Transactions*, vol. 53, pp. 289-297, 2014.
- [23] D. Josephine Sevarani Ruth, K. Dhanalakshmi and S. Sunjai Nakshatharan, "Bidirectional angular control of an integrated sensor/actuator shape memory alloy based system," *Measurement*, vol. 69, pp. 210-221, 2015.
- [24] T. Georges, V. Brailovski and P. Terriault, "Characterization and design of antagonistic shape memory alloy actuators," *Smart Materials and Structures*, vol. 21, pp. 1-8, 2012.
- [25] M. G. Faulkner, J. J. Amalraj and A. Bhattacharyya, "Experimental determination of thermal and electrical properties of Ni-Ti shape memory wires," *Smart Materials and Structures*, vol. 9, pp. 632-639, 2000.
- [26] M. Elahinia and M. Ahmadian, "An enhanced SMA phenomenological model: I. The shortcomings of the existing models," *Smart Materials and Structures*, vol. 14, pp. 1297-1308, 2005.